Institutional Repository

This document is published in:

Fabrication and examination of oxidation resistance of zinc coated copper and brass components by chemical deposition

D. Chaliampalias[1], M. Papazoglou[1], S. Tsipas[2], E. Pavlidou[1], S. Skolianos[2], G. Stergioudis[1] and G. Vourlias*[1]

[1] Physics Department, Aristotle University of Thessaloniki, Thessaloniki 54124, Greece

[2] Department of Mechanical Engineering, Aristotle University of Thessaloniki, Thessaloniki 54124, Greece

* Corresponding author, email gvourlia@auth.gr

Abstract: In this work, the structure and the oxidation resistance of Zn deposited Cu and brass metallic components are examined. The deposition was accomplished with pack cementation chemical deposition. The examination of the samples was performed with electron microscopy and X-ray diffraction analysis. It was found that coatings on Cu substrate consist of two layers with different Zn concentrations, while coatings on brass were single layered with almost constant Zn concentration. The presence of distinct Zn–Cu phases was revealed in both cases. The subjection of the as coated samples together with the uncoated substrates in air at 400ºC showed that both Zn coated samples have enhanced resistivity in such atmospheres, as most of the coating remained mostly unoxidised, and the substrates were fully protected. On the contrary, the bare substrates appear to have undergone severe damage as brittle oxides were formed on their surface.

**Keywords:** Coatings, Zinc, Copper alloys, Pack cementation, Oxidation

Introduction

Cu and Cu alloys have specific properties, such as excellent thermal and electrical conductivity, malleability and ductility, which account for their extensive use as engineering materials. The most common use of Cu is in applications requiring high electrical conductivity.[1] Cu based alloys have been evaluated and used for a wide range of high strength and high thermal conductivity applications at elevated temperatures, while several brasses are also essentially noted for their formability. Furthermore, these materials are corrosion resistant in ambient temperatures compared with pure Cu.[2] Brass components are equally employed in outdoor and indoor applications, such as roofing for building construction, panels, statue parts and art hardware.[3] However, the usage of these materials in aggressive environments is usually limited by severe oxidation attack. When exposed in an elevated temperature environment, a film consisting of Cu_2O and CuO is formed on the surface. At low temperatures (up to 100°C), the oxide film thickness increases logarithmically with time and irregularly at higher temperatures,[2] which result to its progressive crack and spallation. The deposition of a surface coating usually prevents severe material degradation and improves the oxidation resistance of the base metal.[4–6] The Zn–Cu binary phase diagram shows that it is possible to form several intermetallic phases derived from Zn and

Cu. Studies of the above intermetallic compounds have shown that they can be candidate materials for high temperature structural applications.[1]

The most widely used technique to produce protective Zn coating is hot dip galvanising. According to this technique, the substrates under deposition, after a certain preparation of their surface, are immersed in a molten Zn bath, which results in the formation of a thick Zn coating layer. A novel technique that is also suitable for Zn deposition is chemical vapour deposition by pack cementation. In this case, the substrates are packed together with the donor Zn material and a halide salt chemical activator in a ceramic crucible. Then, the packed mixture and substrate are heated in inert atmosphere at deposition temperature. Pack cementation is a novel, relatively simple chemical vapour deposition process, which additionally deposits coatings on any substrate of complex geometry. Moreover, this method shows several advantages, compared to the hot dip galvanising techniques, as it has little environmental impact because no fumes, such as white clouds of ZnO, $ZnCl_2$ and NH_4Cl, which emerged during hot dip galvanising, are formed during the formation of the Zn coating. In addition, the energy consumption during pack cementation is much lower because the deposition is accomplished at lower temperatures.[7]

This work aimed to investigate the structure of Zn coatings deposited on Cu and brass substrates with pack
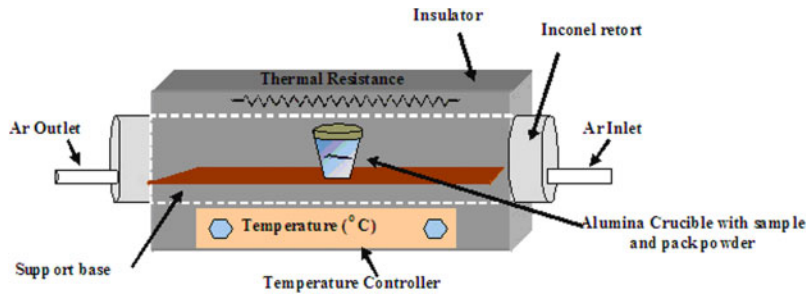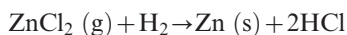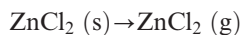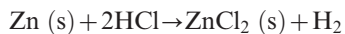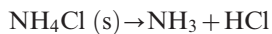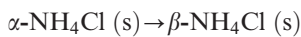
1 Schematic representation of pack cementation deposition set-up

cementation process. Furthermore, an initial assessment of the oxidation resistance of the as coated samples was made by subjecting the coated samples at elevated temperature air environment. The examination was accomplished by microscopic observation and X-ray diffraction (XRD) analysis after the deposition process and after the oxidation tests.

Experimental

In this work, 3 mm thick substrates were used, which were also cleaned and thoroughly degreased with sandblast and sized to 15×10 mm. The substrates were pure Cu and brass (containing 35–45 wt-%Zn). Finally, the substrates were polished up to 600 grid SiC paper and rinsed with dry alcohol in an ultrasonic bath. For the pack cementation deposition process, powders consisted of 1 wt-%NH$_4$Cl halide salt, which was the chemical activator, 40 wt-%Zn coming from laboratory grade Zn powder (99·999%), which was the donor material, and 59 wt-%Al$_2$O$_3$, which was the inert filler material. The cleaned coupons were buried in the pack powder mixture and charged into cylindrical high temperature ceramic crucibles. The filled crucibles were also suitably sealed with ceramic leads. The sealed pack system was inserted in a furnace for ~2 h at ~50°C in order to dry and remove the remaining moisture of the sealer. Finally, the crucibles were placed in a tubular argon purged electric furnace, preheated at 400°C, for 4 h (Fig. 1). The particular experimental parameters were suitably selected according to the experimental procedure followed in previous works for Zn deposition on steel substrates by pack cementation.[7–10] In these references, the chemical mechanism of Zn deposition is analysed thoroughly. Taking under consideration the particular analysis, the deposition mechanism in this case is roughly described by the following chemical reactions

$$\alpha\text{-NH}_4\text{Cl (s)} \rightarrow \beta\text{-NH}_4\text{Cl (s)}$$

$$\text{NH}_4\text{Cl (s)} \rightarrow \text{NH}_3 + \text{HCl}$$

$$\text{Zn (s)} + 2\text{HCl} \rightarrow \text{ZnCl}_2 \text{ (s)} + \text{H}_2$$

$$\text{ZnCl}_2 \text{ (s)} \rightarrow \text{ZnCl}_2 \text{ (g)}$$

$$\text{ZnCl}_2 \text{ (g)} + \text{H}_2 \rightarrow \text{Zn (s)} + 2\text{HCl}$$

After the 4 h deposition, the crucibles were left in the furnace to cool down to ambient temperature without interrupting the Ar flow in order to preserve the inert atmosphere of the process. Some of the as coated samples were then subjected at 400°C in air for 24 h together with the corresponding uncoated substrates in order to evaluate the resistance of the coupons in the particular aggressive conditions. For the examination of the

microstructure, cross-sections from each specimen have been cut, mounted in bakelite, polished down to 5 μm alumina emulsion and then suitably etched. The examination of the coated and oxidised samples was performed with scanning electron microscopy (SEM) using a JEOL 840A SEM (20 kV; JEOL, Tokyo, Japan), while the element distribution was investigated using an ISIS 2000 energy dispersive X-ray analyser (Oxford Instruments, Oxford, UK). Finally, the characterisation of the phases formed in the coatings was accomplished using a two-cycle Philips PW 1050 diffractometer (PANalytical, Almelo, The Netherlands) (Cu K_α radiation) with the Bragg–Brentano geometry (XRD).

Results

Examination of as deposited samples

From the SEM examination of the as deposited samples, it was found that in both cases, a thick coating was formed over the substrate. Some typical cross-sectional micrographs of the as deposited pack coatings are presented in the inset graphs of Fig. 2. From the corresponding cross-sectional SEM images, the coatings are characterised by high homogeneity, as no cracks and porous areas are detected. The thickness of the coating is 100 and 110 μm for the Cu and brass samples respectively. This thickness level is big enough to provide significant isolation of the underlying substrate from aggressive environments and thus enhancing the corrosion resistance of the system.

More analytical examination of the deposited coatings revealed that the coating on the Cu substrate consists of two compact homogeneous layers with different Zn concentrations. Cross-section energy dispersive spectroscopy (EDS) stoichiometric topic analysis showed that the coating is composed only by Zn and Cu. Each layer contains different intermetallic phases from the corresponding binary alloy Cu–Zn phase diagram.[11] Particularly, Zn concentration in the layer located in contact with the Cu substrate (internal) varies between 45·5 and 50·7 wt-%, while in the overlying layer (external), this concentration varies between 57·7 and 70·6 wt-% (Fig. 2a). These results were also confirmed from the corresponding cross-sectional elemental line scanning of the coated samples. The average thickness of these layers was measured to be 60 μm for the internal and 50 μm for the external layer. Furthermore, the coating on brass substrate is single layered with the Zn concentration varying between 57·7 and 70·6 wt-% (Fig. 2b). The average thickness of this layer was measured to be 100 μm. The compositional results are confirmed by the corresponding EDS line scanning graph and are summarised in Table 1.
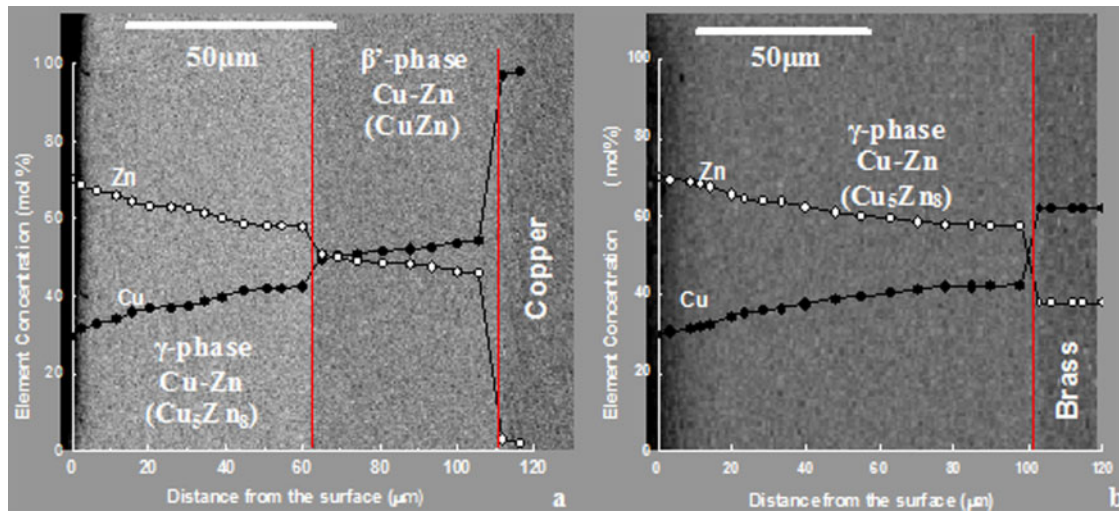
2 Cross-sectional SEM images of coating surface in of *a* Cu and *b* brass substrate together with corresponding compositional profiles (inset graphs)

The formation of both Zn layers is a result of the high diffusivity of Zn atoms in Cu and brass alloys under the particular deposition temperature. Substitutional diffusion took place due to the comparable atomic radius of the elements and the existence of vacancies in Cu and brass crystal lattices. Thus, a strong metallic bond is developed between the coating and the substrates, which enhance the adhesion of the two materials.

The phase composition of the two coatings was examined and identified by XRD analysis (Fig. 3). The XRD peak identification is in absolute agreement with EDS analysis experimental data. Zn coated Cu substrates were found to contain two phases, which correspond to the γ phase (Cu_5Zn_8, 57·7–70·6 wt-%Zn) for the external layer and to the β' phase (CuZn, 45·5–50·7 wt-%Zn) for the internal layer. The coating layer formed on the brass substrate corresponds to the γ phase (Cu_5Zn_8, 57·7–70·6 wt-%Zn) of the Cu–Zn phase diagram. The structure differences are better enlightened in the comparative XRD pattern of Fig. 3, where on Zn coated Cu, two distinct phases are denoted and only one on the brass coupon.[12]

The crystallisation of the β' brass phase forms simple centred cubic cells, which correspond to $Pm\bar{3}m$ space group. The unit cell edge length is between 2·93 and 2·95 Å. Moreover, the crystallisation of the γ phase forms body centred cubic cells, which belong to the $I\bar{4}3m$
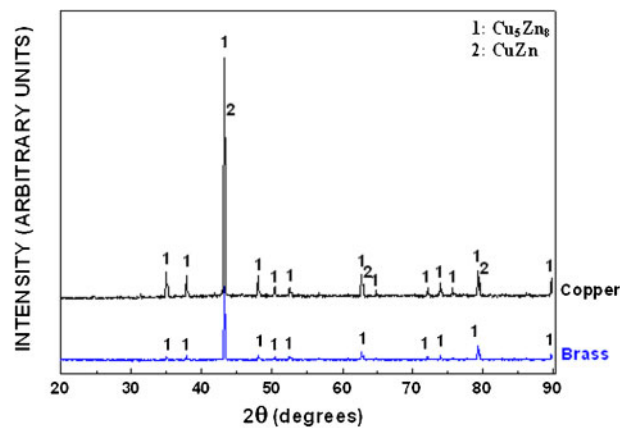
3 X-ray diffraction diagrams of Zn coated Cu and brass substrates: peaks denoted as 1 correspond to Cu_5Zn_8 phase (PDF no. 65-6566), and peaks denoted as 2 correspond to CuZn phase (PDF no. 65-6321)[12]

space group. The unit cell edge length is between 8·85 and 8·89 Å.[12] The structural and crystallographic results of the as formed phases on both substrates are summarised in Table 2.

Diffusion coefficient calculation

The mechanism of the formation of pack cementation depositions is mainly based on the diffusion of the donor material in the substrate. Particularly in the herein examined cases, the Zn atoms diffuse in Cu and brass alloys. Thus, substitutional diffusion takes place, which can be attributed to the comparable atomic radius of the elements and the existence of vacancies in Cu and brass crystal lattices. As a result, a strong metallic bond is developed between different atoms of the coatings and the substrates, which enhance the adhesion of the two materials.

Table 1 Results of EDS analysis of phases in Fig. 1

Substrate	Layer	Zn concentration, wt-%	Phase	Formula
Cu	Internal	45·5–50·7	β'	CuZn
	External	57·7–70·6	γ	Cu_5Zn_8
Brass	Single layer	57·7–70·6	γ	Cu_5Zn_8

Table 2 Structure information for substrates and coatings

	Cu	Brass (*a* + *b* phase Cu–Zn)	β' phase Cu–Zn (CuZn)	γ phase Cu–Zn (Cu_5Zn_8)
Crystal system	Cubic	Cubic, cubic	Cubic	Cubic
Space group	$Fm\bar{3}m$	$Fm\bar{3}m$, $Pm\bar{3}m$	$Pm\bar{3}m$	$I\bar{4}3m$
Cell parameter *a*, Å	3·615	3·615, 2·93–2·95	2·93–2·95	8·85–8·89

3
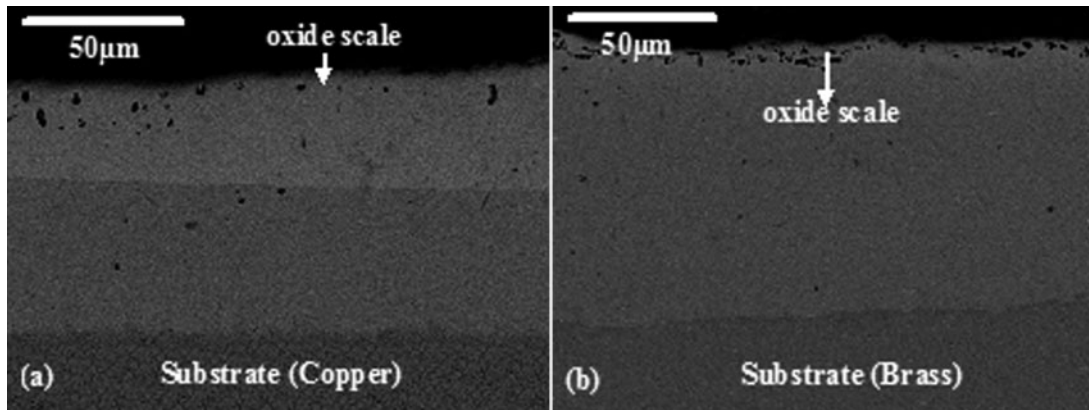
4 Cross-sectional SEM images of oxidised coated *a* Cu and *b* brass substrate
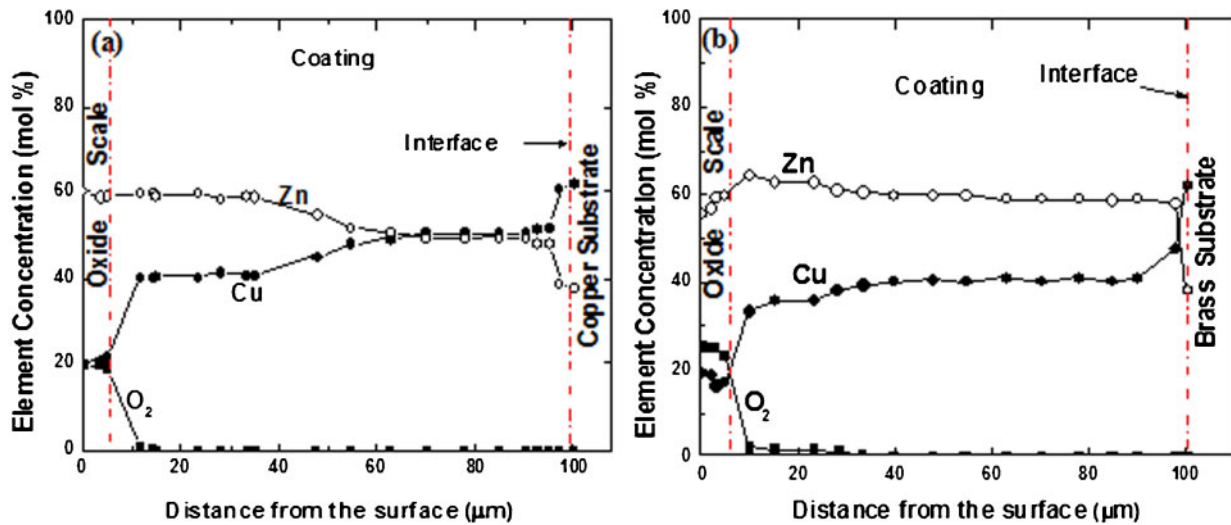
5 Energy dispersive spectroscopy line scanning of oxidised Zn coated *a* Cu and *b* brass

Considering that the deposition rate is proportional to the diffusion coefficient, it is necessary to make the appropriate calculations in order to evaluate the first by determining the second. Both depositions were activated by the particular experimental and chemical conditions described in the experimental part, and so the diffusion coefficient D was calculated using the integrated equation of Fick's second law (equation (1))

$$\frac{\partial C}{\partial t} = D \frac{\partial^2 C}{\partial x^2} \qquad (1)$$

where C is the element concentration, t is the time of the diffusion and x is the diffusion depth measured from the surface.

Before deposition, all the diffusing atoms in the substrate are uniformly solute and distributed having concentration C_0. The value of x at the surface is zero, and while time t is taken to be zero, the instant before the diffusion process begins. By implying these assumptions for the case of semi-infinite crystal, the solution of equation (1) is as described in equation (2)[13]

$$\frac{C_x - C_O}{C_s - C_O} = 1 - \mathrm{erf}(z), \quad z = \frac{x}{2(Dt)^{1/2}} \qquad (2)$$

where C_x is the element concentration at x depth from the surface, C_s is the concentration of the diffused element on the surface and erf (z) is the corresponding error function. The z values for the particular error functions calculated in this case are summarised in Table 3.[14]

Concentrations and diffusion depth were revealed by the SEM images, and the EDS analysis results and are reported in Table 4 together with the as calculated

Table 3 List of *z* values for calculated error functions for both substrates

β′ phase of Cu substrate		Brass substrate	
z	erf (z)	z	erf (z)
1	0·84	0·8	0·74
z	0·85	z	0·77
1·1	0·88	0·9	0·79

Table 4 Diffusion results

	C_s, wt-%	$C_{(x,t)}$, wt-%	C_0, wt-%	x, m	t, s	D, m² s⁻¹
β′ phase of Cu substrate (external layer)	70	0	60	45×10^{-6}	14 400	$6·7 \times 10^{-14}$
Brass substrate	70	60	35	40×10^{-6}	14 400	$3·7 \times 10^{-14}$
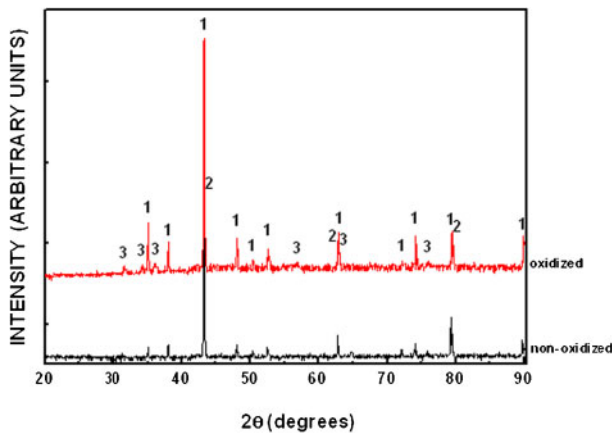
6 Comparative XRD diagrams of Zn coated Cu before and after oxidation: peaks denoted as 1 correspond to Cu_5Zn_8 (PDF no. 65-6566), peaks denoted as 2 correspond to CuZn (PDF no. 65-6321) and peaks denoted as 3 correspond to ZnO (PDF no. 89-1397)[12]

7 Comparative XRD diagrams of Zn coated brass before and after oxidation: peaks denoted as 1 correspond to Cu_5Zn_8 phase (PDF no. 65-6566) and peaks denoted as 2 correspond to ZnO (PDF no. 89-1397)[12]

diffusion coefficient values. The results show the existence of a high diffusion rate of Zn atoms in the Cu and brass substrate, which explains theoretically the formation of thick and compact coatings revealed from the experimental results, which were referred previously.

In both cases of coatings, the diffusion coefficient was found to be of the same magnitude. This is attributed to the similar deposition rates for both substrates. This result is also confirmed from the SEM images, where the total coating thickness is ~100 μm. It is also referred that the coating thickness is proportional to the square root of heating time, and after some time, the thickness of the coating increases with a lower rate until it stops its growth. The existence of two distinct layers in the case of Cu substrate means that after a critical level, the formation of a different phase is favoured.

Corrosion performance

During the oxidation procedure, the coated samples and the corresponding uncoated Cu and brass substrates were exposed for 24 h at 400°C in an aggressive environment. In order to illustrate their situation after oxidation and evaluate their corrosion resistance, the oxidised samples were examined by SEM, while the oxidation products were identified with XRD analysis.

Cross-sectional SEM images of the oxidised samples show that the coatings in both cases were little affected from the particular aggressive environment, as they are found to conserve their initial homogeneity, and only a thin oxide layer is formed on the coating surface (Fig. 4). The uncoated samples, subjected at the same oxidation conditions, suffer from severe degradation caused from the O anion attack. These oxide scales are brittle, which makes them crack successively and effortlessly delaminate from the steel.[15] The Zn containing layer impedes the corrosive elements to reach the substrate, while in some cases, this layer can also act as a sacrificial anode for Cu and brass substrates. Moreover, the oxidation of the coating surface results in the formation of an impermeable oxide scale, which acts as a diffusion barrier to oxidative agents.[16] This scale is formed on the surface, after the reaction of surface elements of the coating with O, and not in the inner areas, which would have a negative effect on the coating
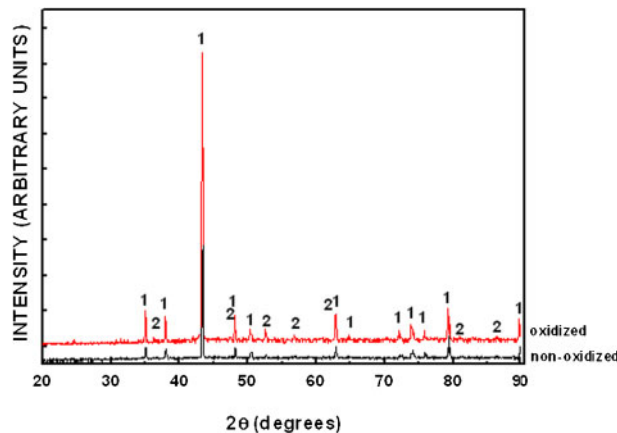
adherence and homogeneity. This is attributed to the growth mechanism of the coating, which is highly affected by the diffusivities of Zn and O through the scale. As it is stated elsewhere,[17–19] Zn diffusivity is many orders of magnitude higher than O diffusivity. Consequently, among the metal cations and the O anions, the migration of the cations takes place much faster through the scale. Thus, the diffusion control results in the growth of the scale at the scale/gas interface, which is very usual for the common base metals.[20]

Point EDS microanalysis performed on both coated coupons revealed that the thickness of the oxide scale in every case was low compared with the total coating thickness. The average scale thickness was measured to be 5 μm. Elemental analysis revealed that the scale areas consist of high concentrations of Zn and Cu atoms together with O (Fig. 5a). The same elemental distribution is found in both coatings, while the underlying part of the coating conserves its primer chemical content as described in the previous paragraph (Fig. 5b). Considering that there is no mixed Zn and Cu oxide reported elsewhere, it can be safely assumed that the scale consisted of Zn or Cu oxides together with the referred Zn–Cu phases tracked in the XRD pattern of Fig. 3.

In order to identify the exact oxidation products that are formed on the coating, the oxidised samples were examined with XRD analysis. In the comparative XRD patterns of the Zn coated Cu substrates (Fig. 6), it is revealed that the diffraction patterns are similar, which is attributed to the coating chemical stability under the particular aggressive conditions. The only difference is the appearance of low intensity ZnO peaks in the pattern of the oxidised sample. These peaks come from the thin oxide film of the surface and have low intensity because of the lower concentration of the oxide compound compared with Cu_5Zn_8 and CuZn in the coating. Thus, Zn amounts are preferably oxidised from the aggressive environment, while Cu protected from ZnO does not react with O.

In the case of the comparative XRD pattern of Zn coated brass (Fig. 7), the two diffraction patterns before and after oxidation are similar, also in this case, as most of the recorded peaks before oxidation, corresponding
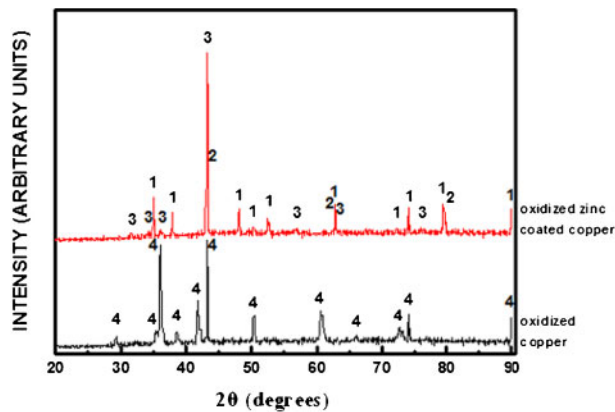
8 Comparative XRD diagrams of Zn coated Cu and Cu substrate after oxidation: peaks denoted as 1 correspond to Cu_5Zn_8 (PDF no. 65-6566), peaks denoted as 2 correspond to CuZn (PDF no. 65-6321), peaks denoted as 3 correspond to ZnO (PDF no. 89-1397) and peaks denoted as 4 correspond to Cu oxides (CuO, Cu_2O and Cu_4O_3; PDF no. 65-3288)[12]

9 Comparative XRD diagrams of Zn coated brass and brass substrate after oxidation: peaks denoted as 1 correspond to Cu_5Zn_8 (PDF no. 65-6566), peaks denoted as 2 correspond to ZnO (PDF no. 89-1397) and peaks denoted as 3 correspond to $Cu_{0.64}Zn_{0.36}$ phase (PDF no. 50-1333)[12]
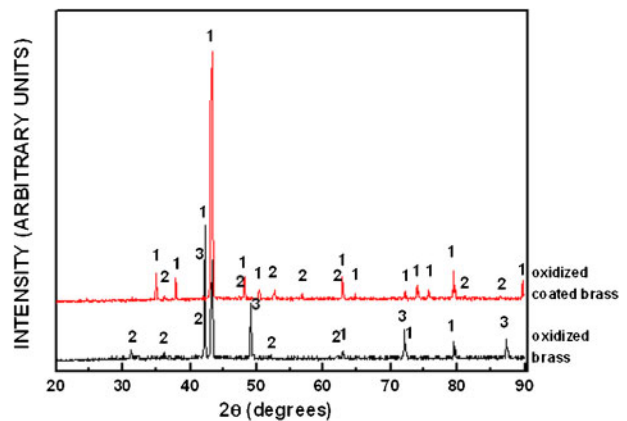
to Cu_5Zn_8, are also present in the corresponding pattern of the oxidised sample. Similarly with the Cu coated samples, in this case, several low intensity ZnO peaks are additionally recorded coming from the passivating thin film formed on the surface of the coating.

From the comparative XRD pattern, where the diffraction peaks of the oxidised coated and uncoated Cu samples are illustrated, the high resistance of the coated surface is distinguished (Fig. 8). On the surface of the Cu substrates, a mix of Cu oxides were identified, which corresponds to CuO, Cu_2O and Cu_4O_3 compounds. These oxides protect the substrate at room temperatures but do not offer equal protection at higher temperatures because they tend to crack and collapse under the effect of the aggressive environment.

On the oxidised brass substrate, no Cu oxides were identified as in the case of Cu specimens (Fig. 9) because there are pre-existing Zn amounts in the substrate, which oxidise more rapidly than Cu and form a protective ZnO film as in the case of Zn coated brass coupons. However, in the case of the untreated specimen, the Zn rich zone underlying below the ZnO film as in the Zn coated samples does not exist. This additional zone offers a longer lasting resistance to similar aggressive environments.

Conclusion

Zn was found to be a well suited metal for protective coatings on Cu and brass substrates. On the as deposited samples, a thick coating was formed as a result of the high diffusivity of Zn atoms in Cu and brass alloys under the particular deposition temperature, which was verified from the diffusivity theoretical calculations. The coating on the Cu substrate consists of two layers, which correspond to the γ phase (Cu_5Zn_8 external layer) and to the β' phase (CuZn internal layer) of the Cu–Zn phase diagram. The Zn coating on the brass substrate is single layered and consists only of the γ phase. The oxidation results showed that both Zn coated samples were found to be unaffected by the particular aggressive environment. This is attributed to the formation of a passivating thin ZnO film on the surface of the coatings and to the high thickness of the as formed depositions, which can provide a long term protection of the substrates when exposed under aggressive environments.

References

1. K. T. Chiang, T. A. Wallace and R. K. Clark: Surf. Coat. Technol., 1996, 86–87, 48–53.
2. P. A. Schweitzer: 'Atmospheric and media corrosion of metals', 2nd edn; 2006, Boca Raton, FL, CRC Press.
3. M. R Bateni, S. Mirdamadi, F. Ashrafizadeh, J. A. Szpunar and R. A. L. Drew: Surf. Coat. Technol., 2001, 199, 192–199.
4. D.Chaliampalias, G.Vourlias, E. Pavlidou,G. Stergioudis and K. Chrissafis: Appl. Surf. Sci., 2009, 255, (12), 6244–6251.
5. D. Chaliampalias, G. Vourlias, E. Pavlidou, S. Skolianos, K. Chrissafis and G. Stergioudis: Appl. Surf. Sci., 2009, 255, (6), 3605–3612.
6. D. Chaliampalias, G. Vourlias, E. Pavlidou, G. Stergioudis, S. Skolianos and K. Chrissafis: Appl. Surf. Sci., 2008, 255, 3104–3111.
7. N. Pistofidis, G. Vourlias, D. Chaliampalias, K. Chrysafis, G. Stergioudis and E. K. Polychroniadis: J. Alloys Compd, 2006, 407, 221–225.
8. G. Vourlias, N. Pistofidis, D. Chaliampalias, E. Pavlidou, G. Stergioudis, E. K.Polychroniadis and D. Tsipas: J. Alloys Compd, 2006, 416, (1–2), 125–130.
9. G. Vourlias, N. Pistofidis, D. Chaliampalias, E. Pavlidou, P. Patsalas, G. Stergioudis, D. Tsipas and E. K. Polychroniadis: Surf. Coat. Technol., 2006, 200, (22–23), 6594–6600.
10. D. Chaliampalias, N. Pistofidis and G. Vourlias: Surf. Eng., 2008, 24, (4), 259–263.
11. ASM International, Alloy Phase Diagrams, Vol. 3, p. 780, American Society of Metals, 1992, New York.
12. 'PC powder diffraction files', JCPDS-ICDD, Newtown Square, PA, USA, 2005.
13. W. D. Callister: 'Materials science and engineering: an introduction', 6th edn; 2006, New York, John Wiley & Sons Inc.
14. A. J. Hayter: 'Probability and statistics for engineers and scientists'; 2001, Cambridge, MA, Duxbury Press.
15. J. R. Davis: 'Copper and copper alloys'; 2001, Materials Park, OH, ASM International.
16. A. R. Marder: Prog. Mater. Sci., 2000, 45, (3), 191–271.
17. J. R. Davis (ed.): 'Heat-resistant materials'; 1997, Materials Park, OH, ASM International.
18. G. W. Tomlins, J. L. Routbort and T. O. Mason: J. Appl. Phys., 2000, 87, 117–123.
19. P. Erhart and K. Albe: Phys. Rev. B, 2006, 73B, 1–9.
20. M. G. Fontana: 'Corrosion engineering', 3rd edn; 1986, New York, McGraw-Hill.